SCIENTIFIC REPORTS

OPEN

Macroscopic phase separation of superconductivity and ferromagnetism in $Sr_{0.5}Ce_{0.5}FBiS_{2-x}Se_x$ revealed by μSR

A. M. Nikitin[1,5], V. Grinenko[2,3], R. Sarkar[2], J.-C. Orain[4], M. V. Salis[1], J. Henke[1], Y. K. Huang[1], H.-H. Klauss[2], A. Amato [4] & A. de Visser[1]

The compound $Sr_{0.5}Ce_{0.5}FBiS_2$ belongs to the intensively studied family of layered BiS_2 superconductors. It attracts special attention because superconductivity at $T_{sc} = 2.8$ K was found to coexist with local-moment ferromagnetic order with a Curie temperature $T_C = 7.5$ K. Recently it was reported that upon replacing S by Se T_C drops and ferromagnetism becomes of an itinerant nature. At the same time T_{sc} increases and it was argued superconductivity coexists with itinerant ferromagnetism. Here we report a muon spin rotation and relaxation study (μSR) conducted to investigate the coexistence of superconductivity and ferromagnetic order in $Sr_{0.5}Ce_{0.5}FBiS_{2-x}Se_x$ with $x = 0.5$ and 1.0. By inspecting the muon asymmetry function we find that both phases do not coexist on the microscopic scale, but occupy different sample volumes. For $x = 0.5$ and $x = 1.0$ we find a ferromagnetic volume fraction of ~8 % and ~30 % at $T = 0.25$ K, well below $T_C = 3.4$ K and $T_C = 3.3$ K, respectively. For x = 1.0 ($T_{sc} = 2.9$ K) the superconducting phase occupies most (~64 %) of the remaining sample volume, as shown by transverse field experiments that probe the Gaussian damping due to the vortex lattice. We conclude ferromagnetism and superconductivity are macroscopically phase separated.

The interplay between superconductivity and magnetism has been a central issue in superconductivity research for several decades now. Especially, the idea that superconductivity and ferromagnetism can occur simultaneously has attracted the attention of researchers throughout the years. Already in 1957 Ginzburg argued a superconducting phase can exist in a ferromagnet when the spontaneous magnetization M_0 is smaller than the lower critical field $\mu_0 H_{c1}$, but also pointed out the "almost complete impossibility in practice, under ordinary conditions, to observe superconductivity in any sort of ferromagnets"[1]. Two years later Anderson and Suhl asserted that a ferromagnetic alignment of spins in a superconductor can occur, but only in a very small domain-like 'cryptoferromagnetic' configuration, where the domain size l_D is smaller than the superconducting coherence length ξ[2]. On the other hand, early experimental work on Gd doped La[3] and $(Ce,Gd)Ru_2$ alloys[4] indicated superconductivity and ferromagnetism are competing phenomena, which was subsequently corroborated by studies of Chevrel phases, such as $ErRh_4B_4$, where superconductivity is expelled when ferromagnetic order sets in[5]. Here the general idea is that the ferromagnetic exchange field impedes the formation of spin-singlet Cooper pairs that is prescribed by the microscopy theory of Bardeen, Cooper and Schrieffer (BCS)[6]. Notwithstanding this restriction, the search for ferromagnetic superconductors continued unremittingly. This resulted in the discovery of perhaps a dozen of remarkable materials in which superconductivity and ferromagnetism exhibit coexistence. However, in most of these systems, superconductivity and ferromagnetism are confined to different crystallographic planes (e.g.

[1]Van der Waals - Zeeman Institute, University of Amsterdam, 1098 XH, Amsterdam, The Netherlands. [2]Institute of Solid State and Materials Physics, Technical University Dresden, 01062, Dresden, Germany. [3]Leibniz Institute for Solid State and Materials Research (IFW), 01069, Dresden, Germany. [4]Laboratory for Muon-Spin Spectroscopy, Paul Scherrer Institute, 5232, Villigen PSI, Switzerland. [5]Present address: Laboratory for Muon-Spin Spectroscopy, Paul Scherrer Institute, 5232 Villigen PSI, Switzerland. Correspondence and requests for materials should be addressed to A.M.N. (email: artem.nikitin@psi.ch) or A.d.V. (email: a.devisser@uva.nl)

$RuSr_2GdCu_2O_8$[7]) and/or to different electron subsystems, i.e. conduction *and* local $4f$ magnetic moments (e.g. $ErNi_2B_2C$[8], $EuFe_2(As,P)_2$[9] and $RbEuFe_4As_4$[10]). Also, some of the systems have metallurgical difficulties (Y_9Co_7[11,12]) or possibly exhibit a form of phase separation (e.g. the electron gas at the $SrTiO_3/LaAlO_3$ interface[13,14]). On the contrary, in a small group of uranium-based correlated metals formed by UGe_2 (under pressure[15]), $URhGe$[16] and $UCoGe$[17], ferromagnetism and superconductivity do coexist on the microscopic scale and are carried by the same $5f$ electrons. This is corroborated by the itinerant nature of the ferromagnetic state. The superconducting transition temperature, T_{sc}, is below the Curie temperature T_C, hence the label superconducting ferromagnets. Superconducting ferromagnets have provided new opportunities to investigate exotic superconductivity. Theoretical work predicts an odd-parity Cooper pair state mediated by longitudinal spin fluctuations[18,19].

In a recent publication, Thakur *et al.*[20] provide evidence that $Sr_{0.5}Ce_{0.5}FBiS_{2-x}Se_x$, with $x = 0.5$ and 1.0, is a new superconducting ferromagnet ($T_{sc} < T_C$). Magnetization measurements for $x \geq 0.5$ signal bulk superconductivity and a small average ordered Ce-moment ($\sim 0.1\ \mu_B$) in the superconducting state, which is in line with itinerant ferromagnetism. This is further substantiated by specific heat measurements for $x = 0.5$ that show the magnetic entropy, S_m, per Ce atom is only 4% of the expected value for trivalent Ce-$4f$ ($J = 5/2$), $S_m = 0.04 \times$ Rln6. Moreover, they report a dual and quite unusual hysteresis loop in the magnetization below T_{sc} corresponding to the coexistence of ferromagnetism and superconductivity. The parent material $Sr_{0.5}Ce_{0.5}FBiS_2$ has a ferromagnetic transition at $T_C = 7.5$ K and superconducts at $T_{sc} = 2.8$ K[21]. Here magnetic order is due to local moments, as evidenced by their magnitude ($\sim 1\ \mu_B$) and the large value of the magnetic entropy $S_m = 0.5 \times$ Rln2, assuming a doublet crystal field ground state ($J = 1/2$). In their recent report on the $Sr_{0.5}Ce_{0.5}FBiS_{2-x}Se_x$ system Thakur *et al.* established that upon replacing S by isovalent Se T_C reduces and T_{sc} is enhanced. At the same time magnetization and specific heat data were interpreted as evidence for the itinerant character of the $4f$-electrons at high Se doping. Consequently they argue magnetic order and superconductivity are carried by the same type of electrons for $x \geq 0.5$. This and the small size of the ordered moment lead them to draw a close parallel between $Sr_{0.5}Ce_{0.5}FBiS_{2-x}Se_x$ and $UCoGe$ as regards the coexistence of superconductivity and itinerant ferromagnetism.

Here we report muon spin relaxation and rotation (μSR) experiments on $Sr_{0.5}Ce_{0.5}FBiS_{2-x}Se_x$ conducted to investigate the coexistence of superconductivity and ferromagnetism on the microscopic scale. μSR is the technique *par excellence* to probe small magnetic moments, as well as to determine the superconducting and magnetic volume fractions in a crystal[22]. The latter information can normally not be extracted from macroscopic measurements such as the magnetization or specific heat. The experiments were performed on two samples with different Se content x: (i) $x = 0.5$, this sample is taken from the same batch as used by Thakur *et al.*[20], and (ii) $x = 1.0$, this sample was synthesized at the University of Amsterdam. We have carried out zero field and transverse field (TF = 10 mT) μSR experiments in the temperature range 0.25–10 K. We detect both the ferromagnetic order and superconductivity. However, by inspecting the muon asymmetry function we conclude these ordered states do not coexist on the microscopic scale, but occupy different sample volumes. For $x = 0.5$ and $x = 1.0$ we find the ferromagnetic volume fraction is ~8% and ~30% at $T = 0.25$ K, *i.e.* well below $T_C = 3.4$ K and $T_C = 3.3$ K, respectively. Transverse field experiments carried out for $x = 1.0$ demonstrate superconductivity ($T_{sc} = 2.9$ K) occupies most, ~64%, of the remaining sample volume, while for $x = 0.05$ this value is ~50%.

Results and Analysis

$Sr_{0.5}Ce_{0.5}FBiSSe$.

A polycrystalline sample was prepared at the University of Amsterdam and characterized by X-ray diffraction, dc magnetization, ac susceptibility, electrical resistivity and specific heat, as shown in Figures S1–S7 in the Supplementary Information (SI) file. The resulting $T_C = 3.3$ K and $T_{sc} = 2.9$ K are in excellent agreement with the values reported by Thakur *et al.* for the same Se content ($x = 1.0$). At $T = 2.0$ K the low-field magnetization data point to a small ordered moment of $\sim 0.2\ \mu_B$/ Ce. By increasing the field the moment grows and saturates in the high field region (9 T) at a large value of $0.9\ \mu_B$/Ce. Ac-susceptibility measurements shows a large diamagnetic signal, which implies a superconducting screening fraction of ~0.7. The superconducting state is further characterized by the electrical resistivity in an applied magnetic field (Fig. S6) and dc-magnetization measurements (Fig. S7). The data were used to extract a lower critical field, $B_{c1} = 0.6$ mT (Fig. S6c), and an upper critical field $B_{c2} = 2.9$ T for $T \rightarrow 0$ (Fig. S6). All in all, these results show our sample has very similar magnetic and superconducting properties as the sample with $x = 1.0$ investigated by Thakur *et al.*[20]. In the following two sections we present the results of the μSR experiments for $x = 1.0$.

Zero field experiments.

The muon (μ$^+$) depolarization in zero field was measured in the temperature range 0.25–10 K. Typical spectra in the time domain are shown in Fig. 1. In the paramagnetic state at $T = 7.5$ K we observe a pronounced μ$^+$ depolarization indicating the presence of slow magnetic fluctuations. The signal has the full experimental asymmetry ($A_{tot} = 0.23$) and accounts for the whole sample volume. Upon cooling to 3.2 K, *i.e.* to just below T_C, an additional rapid depolarization component appears at short times, which we associate with the ferromagnetic phase. This component further develops with decreasing temperature and the corresponding relaxation rate increases and reaches a value of ~18 μs^{-1} at the lowest temperatures. The asymmetry associated with the ferromagnetic phase (Fig. 1c) tells us that it occupies about 30% of the sample volume. This can be put on a firm footing by the analysis of the zero field data with the two-component μ$^+$ depolarization function

$$G(t) = A_{tot}\left[f_{FM}\left(\frac{2}{3}e^{-\lambda_{FM_1}t} + \frac{1}{3}e^{-\lambda_{FM_2}t}\right) + f_{PM}e^{-\lambda_{PM}t}\right].$$

(1)

Here f_{FM} and f_{PM} are the ferromagnetic (FM) and paramagnetic (PM) volume fractions, respectively, and $f_{FM} + f_{PM} = 1$. λ_{PM} is the relaxation rate in the paramagnetic phase, and λ_{FM_1} and λ_{FM_2} are the fast (2/3 component) and slow (1/3 component) relaxation rates in the ferromagnetic phase, respectively. When fitting the ferromagnetic contribution we fixed λ_{PM} at 0.15 μs^{-1} and fixed the total asymmetry $A_{tot} = 0.23$. We remark this value of λ_{PM} is
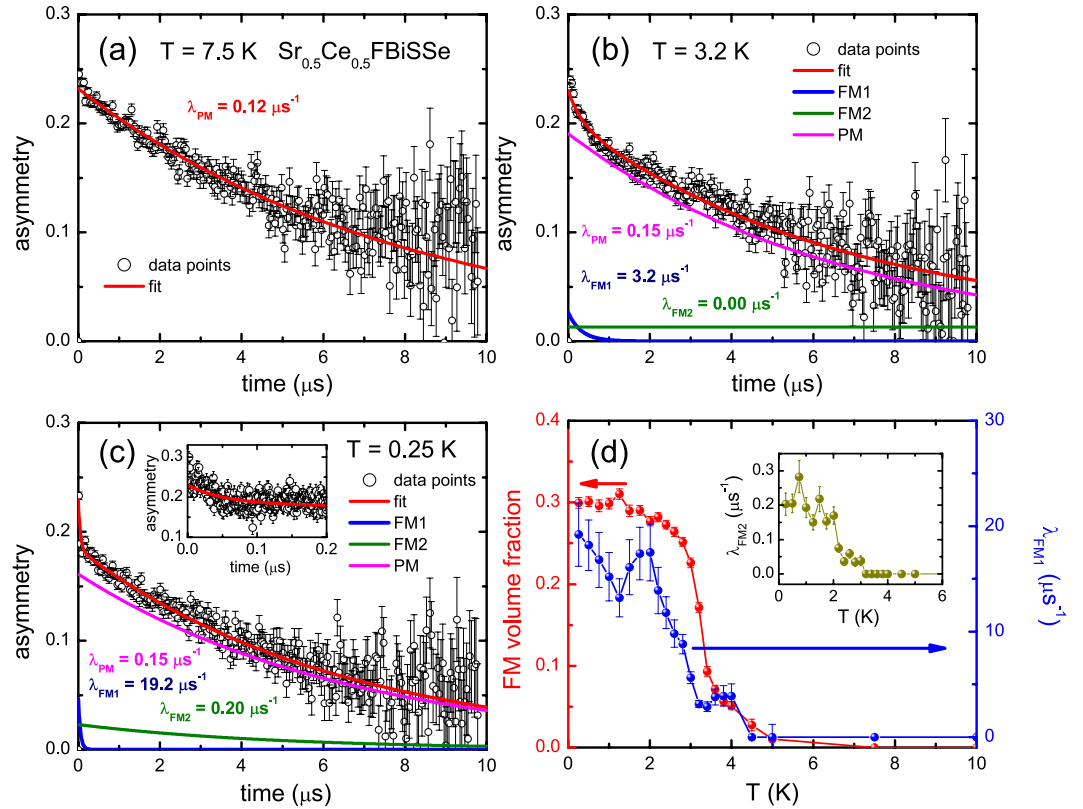
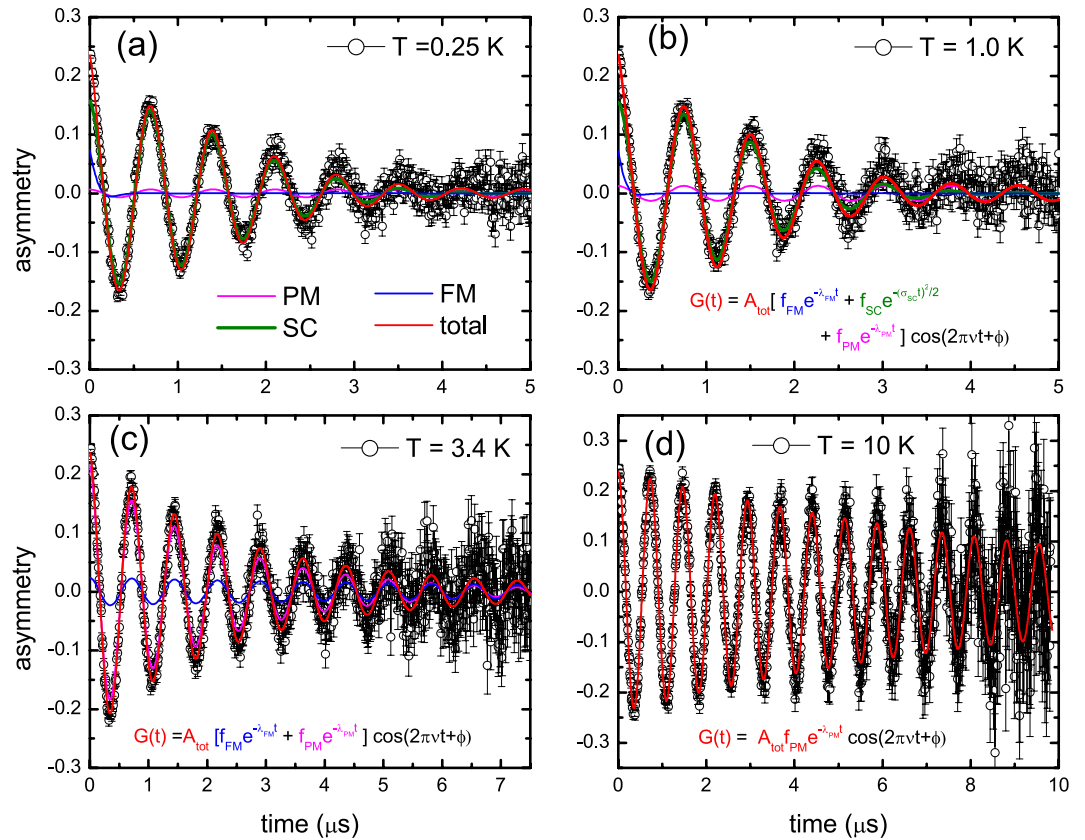**Figure 1.** Zero field μSR data measured for $Sr_{0.5}Ce_{0.5}FBiSSe$. Panels (a–c): asymmetry as a function of time at temperatures of 7.5 K, 3.2 K and 0.25 K, respectively. The red lines are fits to the muon depolarization function eq. 1. The blue, magenta and green lines are the contributions from the ferromagnetic fast (FM$_1$), ferromagnetic slow (FM$_2$), and paramagnetic (PM) signals, respectively. The corresponding relaxation rates are listed. Inset panel (c): asymmetry at $T = 0.25$ K up to 0.2 μs. Panel (d): temperature variation of the ferromagnetic volume fraction f_{FM} (red symbols, left axis) and λ_{FM_1} (blue symbols, right axis). Inset: temperature variation of λ_{FM_2}.

slightly larger than the value extracted at 7.5 K (see Fig. 1a), which indicates it has a weak temperature variation. The results of this fitting procedure at 3 typical temperatures are shown in Fig. 1a,b,c. In Fig. 1d we show the temperature variation of f_{FM} and of the relaxation rates λ_{FM_1} and λ_{FM_2}. Clearly, f_{FM} shows the strongest increase at $T_C = 3.2$ K and then levels off to a ferromagnetic volume fraction of 30%. Correspondingly, λ_{FM_1} and λ_{FM_2} increase and saturate in the ferromagnetic phase. We remark the ratio of the fast and slow relaxation rates is large, $\lambda_{FM_1}/\lambda_{FM_2} \approx 100$.

Transverse field experiments. Transverse field μSR measurements were carried out in a small magnetic field of 10 mT in the temperature range 0.25–10 K. Typical spectra are shown in Fig. 2. In the paramagnetic phase a sizeable damping is observed with an exponential relaxation rate $\lambda_{PM} = 0.10$ μs^{-1} at 10 K. This value compares well to the value found in the zero field experiments. Upon approaching the Curie point the damping increases considerably, as shown in the spectrum at $T = 3.4$ K (Fig. 2c), while by further cooling to below T_{sc} additional damping due to the flux line lattice appears (Fig. 2a,b). Good fits to the transverse field μSR spectra are obtained with the three-component depolarization function

$$G(t) = A_{tot}\left[f_{SC}\,e^{\frac{-(\sigma_{SC}t)^2}{2}} + f_{FM}\,e^{-\lambda_{FM}t} + f_{PM}\,e^{-\lambda_{PM}t}\right]\cos(2\pi\nu t + \phi),\tag{2}$$

where f_{SC} is the superconducting volume fraction and the Gaussian damping due to the vortex lattice is expressed by the relaxation rate σ_{SC}. The parameters $f_{FM}, f_{PM}, \lambda_{FM}$ and λ_{PM} have the same meaning as in the zero-field case. The muon precession frequency is given by ν and its phase by ϕ. When analyzing the spectra at the lowest temperatures we first used eq. 2 with the first two terms only ($f_{PM} = 0$). This irrevocably showed that close to 30% of the sample exhibits ferromagnetic order, as was deduced from the zero field experiment, while superconductivity occupies the remaining sample volume. We remark a slightly better fit was obtained by allowing for an additional small paramagnetic volume fraction with relaxation rate $\lambda_{PM} = 0$ which accounts for 6% of the sample volume, $f_{PM} = 0.06$ (see Fig. 2a). In this case f_{SC} amounts to 0.64. This small paramagnetic volume fraction is attributed to the impurity phase detected in the X-ray diffraction pattern. Next, in order to follow the temperature variation of the fit parameters of the different components we used the following constraints: (i) $f_{FM}(T)$ is taken equal to
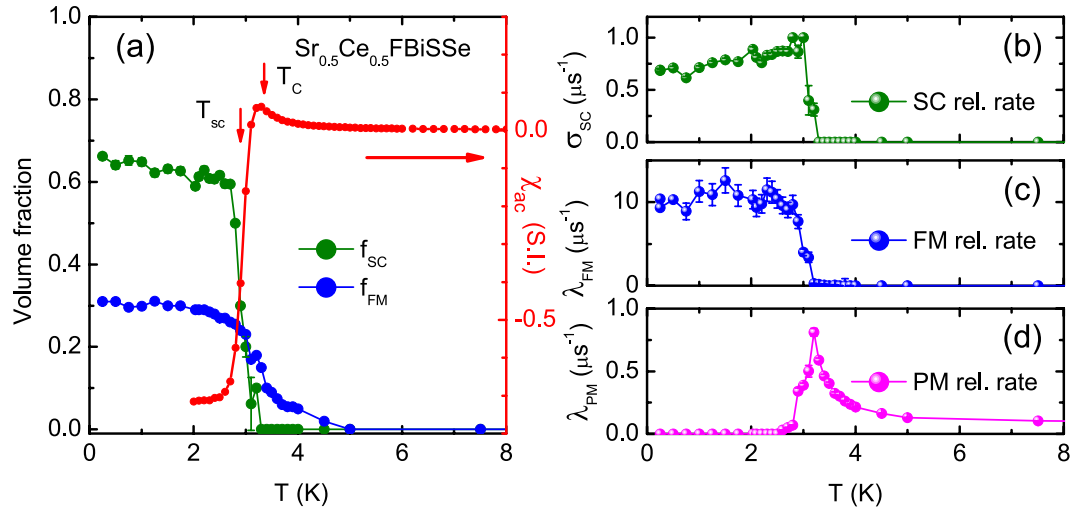
Figure 2. Transverse field μSR data measured for $Sr_{0.5}Ce_{0.5}FBiSSe$. The applied field is $B = 10$ mT. Panels (a–d): asymmetry as a function of time at temperatures of 0.25 K, 1.0 K, 3.4 K and 10 K. The red lines are fits to the muon depolarization function eq. 2. The blue, magenta and green lines are the contributions from the ferromagnetic (FM), paramagnetic (PM) and superconducting (SC) signals, respectively. The muon depolarization functions of the contributing components are listed.

the values obtained in zero field (Fig. 1d), (*ii*) $\lambda_{PM} = 0$ for $T < 2$ K, and (*iii*) $\sigma_{SC} = 0$ for $T > 3$ K. The resulting fit parameters are shown in Fig. 3. For $T \to 0$ $\lambda_{FM} \approx 10 \, \mu s^{-1}$ attains a large value like in the zero field experiment. The superconducting state is characterized by a Gaussian damping with $\sigma_{SC} = 0.70 \, \mu s^{-1}$ for $T \to 0$. Upon increasing the temperature λ_{FM} shows a smooth temperature variation and drops to zero at T_C. On the other hand σ_{SC} first increases with increasing temperature and then drops to zero at T_{sc}. We remark this non-BCS increase is an artefact of the fitting procedure close to T_{sc}. Since $T_{sc} \approx T_C$ it is difficult to disentangle the three components in the vicinity of the phase transitions. $f_{FM}(T)$ and $f_{SC}(T)$ are traced in Fig. 3a. For comparison we have plotted in the same figure the ac-susceptibility measured on a piece of the same $x = 1.0$ batch (see also Fig. S5). The smooth variation of $f_{FM}(T)$ and $f_{SC}(T)$ to zero is in good agreement with $T_C = 3.3$ K and $T_{sc} = 2.9$ K extracted from the magnetic measurements.

$Sr_{0.5}Ce_{0.5}FBiS_{1.5}Se_{0.5}$. A polycrystalline sample with $x = 0.5$ was taken from the same batch as used in ref.[20]. The $x = 0.5$ compound has been characterized extensively by resistivity, ac-susceptibility, magnetization and specific heat measurements[20] (see also SI). DC magnetization measurements in an applied field of 1 mT were used to determine the transition temperatures $T_C = 3.5$ K and $T_{sc} = 2.7$ K. A small spontaneous moment was found with magnitude ~0.09 μ_B/Ce at $T = 2$ K. Furthermore, the analysis of the specific heat data pointed to a low value for the magnetic entropy $S_m = 0.04 \times R\ln 2$ associated with the ferromagnetic transition. The small value of the ordered moment and the reduced entropy were taken as evidence for the development of itinerant magnetism upon replacing S by Se.

Zero field experiments. Zero field μSR time spectra were taken in the temperature interval 0.25–10 K. The data at a few selected temperatures are shown in Fig. 4. In the paramagnetic state the muon depolarization is an exponential function of time with a similar relaxation rate as for $x = 1.0$. At $T = 0.25$ K, deep in the magnetic phase, an additional depolarization mechanism appears at small times ($t < 0.1 \, \mu s$) (see also the inset in Fig. 4a), but it is not as pronounced as for $x = 1.0$. An elaborate analysis showed it is due to a magnetic volume fraction of ~0.08 only. Best fits were obtained by using a two component depolarization function with: (*i*) fast relaxation due to a (disordered) ferromagnetic phase and (*ii*) exponential relaxation in the non-ferromagnetic part due to dilute magnetic impurities[23]:

Figure 3. Fit parameters of the analysis of the transverse field μSR data measured for $Sr_{0.5}Ce_{0.5}FBiSSe$. Panel (a): temperature variation of the ferromagnetic f_{FM} (blue symbols) and superconducting f_{SC} (green symbols) volume fractions (left axis), and the ac-susceptibility (red symbols, right axis). T_{sc} and T_C extracted from χ_{ac} are indicated by arrows. Panels (b–d): temperature variation of the Gaussian damping rate due to superconductivity, and the exponential relaxation rates of the ferromagnetic and paramagnetic phases, respectively.
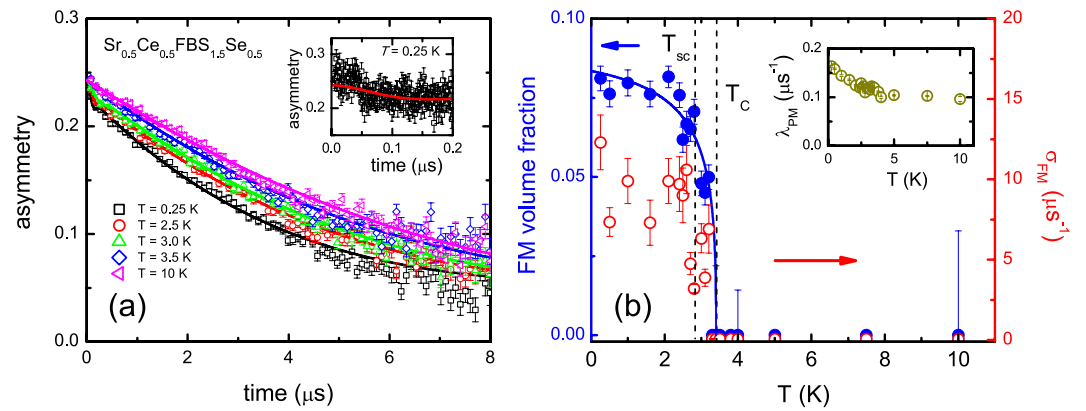
Figure 4. Zero field μSR data for $Sr_{0.5}Ce_{0.5}FBiS_{1.5}Se_{0.5}$. Panel (a): asymmetry as a function of time at temperatures as indicated. The solid lines are fits to eq. 3. The inset shows the asymmetry function at $T = 0.25$ K up to $0.2\,\mu s$. Panel (b): temperature variation of the ferromagnetic volume fraction f_{FM} (blue symbols, left axis) with the solid blue line as a guide to the eye, and σ_{FM} (red symbols, right axis). The vertical dashed lines indicate T_C and T_{sc} from dc-susceptibility measurements (see Fig. S8). Inset: temperature variation of λ_{PM}.

$$G(t) = A_{tot}\left[f_{FM}\left(\frac{1}{3} + \frac{2}{3}[1 - (\sigma_{FM}t)^2]e^{\frac{-(\sigma_{FM}t)^2}{2}}\right) + f_{PM}\left(\frac{1}{3} + \frac{2}{3}[1 - (\sigma_N t)^2 - \lambda_{PM}t]e^{-\left(\frac{(\sigma_N t)^2}{2} - \lambda_{PM}t\right)}\right)\right]$$

(3)

Here f_{FM} and $f_{PM} = 1 - f_{FM}$ are the ferromagnetic (FM) and paramagnetic (PM) volume fractions respectively, σ_{FM} is the ferromagnetic relaxation rate, λ_{PM} is the paramagnetic relaxation rate, and σ_N is the nuclear contribution which was fixed at $0.07\,\mu s^{-1}$. The fit results are shown by the solid lines in Fig. 4a. The temperature variation of f_{FM}, σ_{FM} and λ_{PM} is reported in Fig. 4b. The analysis clearly shows the ferromagnetic phase is bound to a volume fraction of ~0.08 only.

Discussion and Concluding Remarks

The μSR data irrevocably show that the magnetism associated with the ordering temperatures $T_C = 3.4$ K and $T_C = 3.3$ K for $x = 0.5$ and $x = 1.0$, respectively, develops in a part of the sample only. This tells us that substituting Se for S in $Sr_{0.5}Ce_{0.5}FBiS_2$ results in electronic phase separation. Moreover, our μSR analysis with large magnetic relaxation times points to a considerable amount of disorder in the magnetic phase. We stress that our conclusions are robust and do not depend on details of the fitting procedure used. These results sharply contrast with μSR spectra measured for the superconducting itinerant ferromagnet UCoGe with $T_{sc} = 0.5$ K and $T_C = 3.0$ K[24].

In this case a spontaneous muon precession frequency of 2 MHz ($T \rightarrow 0$) was observed below T_C and magnetism was found to be present in the whole sample volume. The itinerant nature of ferromagnetism in UCoGe is underpinned by the small spontaneous moment of 0.03 μ_B per U atom. The observation that magnetism in $Sr_{0.5}Ce_{0.5}FBiS_{2-x}Se_x$ for $x \geq 0.5$ is bound to a reduced sample volume also tells us that the small ordered moments measured for $x = 0.5$[20] and $x = 1.0$ (see SI) are not intrinsic. This naturally explains the 'itinerant' behaviour extracted from the magnetization data. In the case of $x = 1.0$ the measured moment of ~ 0.2 μ_B can be accounted for by a sizeable ordered Ce moment of ~ 0.7 μ_B in 30% of the sample volume. Concurrently, a rough estimate for the magnetic entropy (see SI) associated with the magnetic volume fraction is $1.3 \times$ Rln2 (at $T = 10$ K). Thus magnetism keeps its local moment behaviour upon Se doping.

In the case of $x = 1.0$ the analysis of the transverse field data shows the superconducting phase occupies most of the remaining non-magnetic sample volume of ~64% (see Fig. 3a). This value agrees well with the superconducting screening fraction deduced from the ac-susceptibility measurements (see Fig. S5). From the pronounced damping σ_{SC} in the superconducting state we can calculate the London penetration depth λ with help of the relation $\lambda^2 \approx 0.0609 \gamma_\mu \Phi_0 / \sigma_{SC}$[22]. Here γ_μ is the muon gyromagnetic ratio ($\gamma_\mu / 2\pi = 135.5$ MHz/T) and Φ_0 is the flux quantum. With $\sigma_{SC} = 0.70$ μs^{-1} we calculate $\lambda = 390$ nm for $T \rightarrow 0$. We have also taken transverse field μSR spectra for the $x = 0.5$ compound at a few selected temperatures (see Fig. S9 in SI). The data demonstrate superconductivity develops in about 50% of the sample volume only, while about 40% of the sample is not magnetic and not superconducting even at the lowest temperature $T = 0.25$ K.

Notwithstanding our results, the coexistence of superconductivity and ferromagnetism in BiS_2-based materials such as $Sr_{0.5}Ce_{0.5}FBiS_2$[21] and $CeO_{0.3}F_{0.7}BiS_2$[25] is a remarkable observation and deserves to be studied in detail, notably as regards the possible interplay of local moment magnetism and superconductivity. An important question that has not been answered for these two compounds yet is the one of electronic phase homogeneity, which calls for μSR experiments. Our μSR study on $Sr_{0.5}Ce_{0.5}FBiS_2$ doped with Se irrevocably shows ferromagnetism and superconductivity are phase separated. It provides an excellent example of the power of the μSR technique in condensed matter physics.

Methods

Muon spin relaxation and rotation experiments were carried out with the Multi Purpose Surface Muon Instrument DOLLY installed at the πE1 beamline at the SμS facility of the Paul Scherrer Institute (PSI) in Villigen (Switzerland). The μSR technique makes use of spin-polarized muons implanted in a sample and the ensuing asymmetric decay process into positrons[26]. The positrons are collected in detectors at positions forward and backward with respect to the initial muon spin direction. The muon asymmetry $A(t)$ is determined by calculating

$$A(t) = (N_B(t) - \alpha N_F(t))/(N_B(t) + \alpha N_F(t)),$$

where $N_B(t)$ and $N_F(t)$ are the numbers of positrons detected in the backward and forward detector, respectively, and α is a constant for calibration purposes. The asymmetry function contains detailed information about the spatial distribution of local magnetic fields and their nature, e.g. static or fluctuating. By fitting $A(t)$ to model expressions evaluated for different muon relaxation processes[23] the magnetic properties of the sample can be determined on the microscopic scale. Zero field (ZF) and transverse field (TF) μSR time spectra were recorded in the longitudinal mode, i.e. with the muon spin parallel to the beam direction. In the TF configuration a small magnetic field was applied perpendicular to the beam direction. The samples were attached with General Electric (GE) varnish to the cold finger of a Heliox insert (Oxford Instruments) that allowed for measurements down to $T = 0.25$ K. The sample area for the incident muon beam was typically 100 mm^2. The μSR time spectra were analysed with the software package Musrfit[27] developed at the PSI.

A polycrystalline compound with composition $Sr_{0.5}Ce_{0.5}FBiSSe$ was obtained by the solid state synthesis procedure as described in ref.[20]. Ce_2S_3, Bi_2S_3, SrF_2, Bi and Se were thoroughly mixed, pelletized and sealed in a quartz tube under vacuum. The tubes were then heated twice at 800 °C for 24–36 hours with an intermediate grinding. The sample of the $Sr_{0.5}Ce_{0.5}FBiS_{1.5}Se_{0.5}$ compound comes from the same batch as used in ref.[20]. Magnetization, ac-susceptibility, electrical resistivity and specific heat measurements reported in the Supplementary information were carried out in a Physical Property Measurement System equipped with a 9 T superconducting magnet (Quantum Design).

Data availability. The data needed to evaluate the conclusions in the paper are presented in the paper and the Supplementary Information. Additional information may be requested from the authors.

References

1. Ginzburg, V. L. Ferromagnetic superconductors. *Sov. Phys. JETP* **4**, 153–160 (1957).
2. Anderson, P. W. & Suhl, H. Spin alignment in the superconducting state. *Phys. Rev.* **116**, 898–900 (1959).
3. Matthias, B. T., Suhl, H. & Corenzwit, E. Spin exchange in superconductors. *Phys. Rev. Lett.* **1**, 92–94 (1958).
4. Matthias, B. T., Suhl, H. & Corenzwit, E. Ferromagnetic superconductors. *Phys. Rev. Lett.* **1**, 449–450 (1958).
5. Fertig, W. A. *et al*. Destruction of superconductivity at the onset of long-range magnetic order in the compound ErRh$_4$B$_4$. *Phys. Rev. Lett.* **38**, 987–990 (1977).
6. Berk, N. F. & Schrieffer, J. R. Effect of ferromagnetic spin correlations on superconductivity. *Phys. Rev. Lett.* **17**, 433–435 (1966).
7. Bernhard, C. *et al*. Coexistence of ferromagnetism and superconductivity in the hybrid ruthenate-cuprate compound RuSrGdCu$_2$O$_8$ studied by muon spin rotation and dc magnetization. *Phys. Rev. B* **59**, 14099–14107 (1999).
8. Canfield, P. C., Bud'ko, S. L. & Cho, B. K. Possible co-existence of superconductivity and weak ferromagnetism in ErNi$_2$B$_2$C. *Physica C: Superconductivity* **262**, 249–254 (1996).
9. Liu, Y. *et al*. Superconductivity and ferromagnetism in hole-doped RbEuFe$_4$As$_4$. *Phys. Rev. B* **93**, 214503 (2016).
10. Cao, G. *et al*. Superconductivity and ferromagnetism in EuFe$_2$(As,P)$_2$. *Journal of Physics: Condensed Matter* **23**, 464204 (2011).
11. Bochenek, L., Rogacki, K., Kołodziejczyk, A. & Cichorek, T. *d*-band metal Y$_9$Co$_7$ revisited: Evidence for local coexistence of superconductivity and itinerant ferromagnetism. *Phys. Rev. B* **91**, 235314 (2015).

12. Larson, J. *Quantum phase transitions in CoCl₂ salts, and the nature of the co-existence of magnetism and superconductivity in Y₉Co₇ and La₂₋ₓSrₓCuO₄₊ᵧ.* Ph.D. Thesis, Technical University of Denmark, 2013.
13. Bert, J. A. *et al.* Direct imaging of the coexistence of ferromagnetism and superconductivity at the LaAlO₃-SrTiO₃ interface. *Nat. Phys.* **7**, 767–771 (2015).
14. Shen, S. *et al.* Observation of quantum Griffiths singularity and ferromagnetism at the superconducting LaAlO₃/SrTiO₃ (110) interface. *Phys. Rev. B* **94**, 144517 (2016).
15. Saxena, S. S. *et al.* Superconductivity on the border of itinerant-electron ferromagnetism in UGe₂. *Nature (London)* **406**, 587 (2000).
16. Aoki, D. *et al.* Coexistence of superconductivity and ferromagnetism in URhGe. *Nature (London)* **413**, 613 (2001).
17. Huy, N. T. *et al.* Superconductivity on the border of weak itinerant ferromagnetism in UCoGe. *Phys. Rev. Lett.* **99**, 067006 (2007).
18. Fay, D. & Appel, J. Coexistence of *p*-state superconductivity and itinerant ferromagnetism. *Phys. Rev. B* **22**, 3173–3182 (1980).
19. Monthoux, P., Pines, D. & Lonzarich, G. G. Superconductivity without phonons. *Nature* **450**, 1177–1183 (2007).
20. Thakur, G. S. *et al.* Coexistence of superconductivity and ferromagnetism in Sr₀.₅Ce₀.₅FBiS₂₋ₓSeₓ (x = 0.5 and 1.0), a non-U material with $T_c < T_{FM}$. *Scientific Reports* **6**, 37527 (2016).
21. Li, L. *et al.* Coexistence of superconductivity and ferromagnetism in Sr₀.₅Ce₀.₅FBiS₂. *Phys. Rev. B* **91**, 014508 (2015).
22. Amato, A. Heavy-fermion systems studied by μSR technique. *Rev. Mod. Phys.* **69**, 1119–1180 (1997).
23. Yaounc, A. & D de Réotier, P. *Muon spin rotation, relaxation and resonance; applications to condensed matter.* (Oxford University Press, Oxford, 2011).
24. de Visser, A. *et al.* Muon spin rotation and relaxation in the superconducting ferromagnet UCoGe. *Phys. Rev. Lett.* **102**, 167003 (2009).
25. Lee, J. *et al.* Coexistence of ferromagnetism and superconductivity in CeO₀.₃F₀.₇BiS₂. *Phys. Rev. B* **90**, 224410 (2014).
26. Blundell, S. J. Spin-polarized muons in condensed matter physics. *Contemp. Phys.* **40**, 175–192 (1999).
27. Suter, A. & Wojek, B. Musrfit: A free platform-independent framework for μSR data analysis. *Physics Procedia* **30**, 69–73 (2012).

Acknowledgements

Author Contributions

A.M.N., V.G., R.S., J.-C.O. and A.d.V. conducted the μSR experiments and analysed the data. M.S. carried out magnetization, ac-susceptibility and electrical resistivity measurements. J.H. carried out specific heat measurements. Y.K.H. synthesized the x = 1.0 compound. H.-H.K. and A.A. supervised the μSR experiments. A.M.N. and A.d.V. wrote the manuscript with help of V.G. and R.S. All authors reviewed the manuscript.

Additional Information

Supplementary information accompanies this paper at https://doi.org/10.1038/s41598-017-17637-y.

Competing Interests: The authors declare that they have no competing interests.

Publisher's note: Springer Nature remains neutral with regard to jurisdictional claims in published maps and institutional affiliations.